ISSN 2007-9737

Fast and Efficient Palmprint Identification of a Small Sample within a Full Image

Carlos Francisco Moreno-García and Francesc Serratosa

Universitat Rovira i Virgili, Departament d'Enginyeria Informàtica i Matemàtiques, Spain

carlosfrancisco.moreno @estudiants.urv.cat; francesc.serratosa@urv.cat

Abstract. In some fields like forensic research, experts demand that a found sample of an individual can be matched with its full counterpart contained in a database. The found sample may present several characteristics that make this matching more difficult to perform, such as distortion and, most importantly, a very small size. Several solutions have been presented intending to solve this problem, however, big computational effort is required or low recognition rate is obtained. In this paper, we present a fast, simple, and efficient method to relate a small sample of a partial palmprint to a full one using elemental optimization processes and a voting mechanic. Experimentation shows that our method performs with a higher recognition rate than the state of the art method, when trying to identify palmprint samples with a radius as small as 2.64 cm.

Keywords. Sub-image registration, Hough method, candidate voting, Hungarian algorithm.

1 Introduction

1.1 Problem Definition

Image registration in computer vision tries to determine which parts of one image correspond to which parts of another image. This problem often arises at the early stages of many computer vision applications such as scene reconstruction, object recognition and tracking, pose recovery, and image retrieval. Interesting image registration surveys are [1, 2], which explain the problematic of this goal. It is of basic importance to develop effective methods that are robust in two aspects: a) being able to deal with noisy measurements, and b) having a wide field of application.

The two typical steps involved in the solution of the image registration problem are the following [3]. First, some salient points are selected from both images [4], and then a set of tentative matches between these sets of points is computed [5, 6, 7]. Second, these tentative matches can be further refined by a process of outlier rejection [8] that eliminates the spurious correspondences or, alternatively, they can be used as a starting point of some optimization scheme to find a different and more consistent set [9]. Recently, other methods have appeared which take into consideration salient points grouped in several sets of points, since they assume different transformations are applied to each point set [10]. Moreover, some methods have been presented which register several images at a time [11] to increase the probability of finding successful matches.

The main drawback of all these methods is that their ability to obtain a dense correspondence set strongly depends on the reliability of tentative correspondences. In some image-registration based applications (forensic palmprint recognition, satellite images, etc.), it is more usual to detect a tiny partial image rather than a full sample. In these cases, tentative initial correspondences returned by the first step fail due to a great amount of outliers that have to be detected while comparing a tiny image to a full image. Thus, the second step (usually highly dependent on these initial correspondences) is able to recover neither the correct correspondences nor the transformation matrix from the tiny image to the large image.

1.2 State of the Art

Several methods have been presented for palmprint recognition, which are collected in surveys such as [12, 13]. An initial approach

modeled by [14] proposed a novel algorithm for minutiae matching using crease elimination. Later, [15] proposed a low resolution image matching based on palmprint ridges. Both of these models cannot be applied while performing partial to full palmprint matching since they specifically consider full to full image alignment.

Although several proposals have been developed in the meantime, it is not until the work of [16] where we observe a broad study on latent palmprint matching, resulting in a full to full and a partial to full matching system based on Gabor filters and Active Contour Model, using exclusively minutiae matching. Although there is an improvement in recognition rates for full to full scenarios, the partial to full algorithm obtains inferior results. Moreover, the tests are done using "synthetic" and "pseudo-latent" samples. This means that partial samples are not obtained from a separate source, but rather adapted from the full ones. Additionally, this method requires a partial sample to be composed of at least 70% of the palm, whereas in forensic scenarios this is not always feasible.

A year later, [17] proposed a latent palmprint matching technique consisting of partial to full palmprints for forensic applications, improving the feature extraction algorithm proposed in [16]. In spite of the appropriateness of this approach, we encounter the problem of large computational demand on Discrete Fourier Transform and Gabor Filtering, and additionally an apparent requirement of about 150 minutiae per partial palmprint. To achieve an acceptable classification rate, a fusion of multiple partial palmprints is needed from the same palmprint. This is an important demand, since sometimes only one sample is available.

More recent approaches propose different matching criteria than merely minutiae analysis. A document presented by [18] proposes a multi-feature fusion algorithm that, compared to the latent matching elaborated by Jain and Feng, presents an improved matching percentage of 91.7%; however, the method is not presented for partial to full matching. [19] proposed a robust ridge-based matching algorithm which outperforms the techniques presented in [17, 18]. However, it is again unclear if the method works for partial palmprints and, since it's based on more features than the minutiae, it requires a higher definition and quality than images found on, for example, a crime scene. A method based on wavelets has just been presented [20]; although it obtained interesting results, this method does not work on partial palmprints due to the need of representing the whole ridges. Nibouche *et al.* presented a method to obtain a fingerprint distance [21], but it needs several samples of the same full palmprint since it is based on Principal Component Analysis (PCA). In [22], PCA are also used, but each palmprint is divided into several square-overlapping blocks. This was done to classify these blocks into either a good block or a non-palmprint block. Finally, in the paper presented by [23], palmprint images are decomposed by 2D Gabor wavelets. The drawback of this methodology is that this decomposition is very sensitive to the length of the obtained palmprint, and again cannot be used to satisfy our requirements.

While most of the palmprint matching approaches are based on a full to full association, our contribution is based on a tiny partial section of the palmprint being associated with its complete counterpart (and only one sample is available), which is a more plausible scenario in forensics studies. Only methods presented in [16, 17] considered this fact, although they need a larger partial palmprint than our requirements. Although we observe that methods tend to include more aspects of the palm rather than just the minutiae, we consider that, in order for our algorithm to keep a low computational complexity, it is more optimal to use exclusively this feature.

In this paper, we present an image registration method that explicitly considers that one of the images is noisy and small, and the other is a full image in a dataset. The paper is organized as follows. In Section 2, we describe the method. In Section 3, we explain how we applied our method to a partial palmprint registration case. Finally, we conclude the paper in Section 4.

2 Methodology

Consider we want to align a small image to a large image. We suppose the small one shows part of the larger one. For this reason, we say the

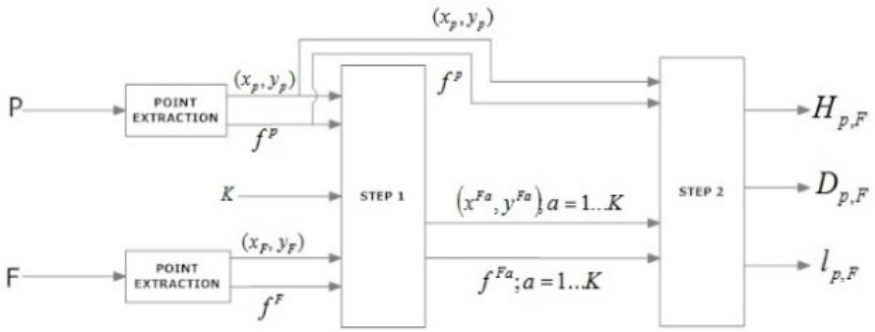

Fig. 1. Diagram of the Registration method

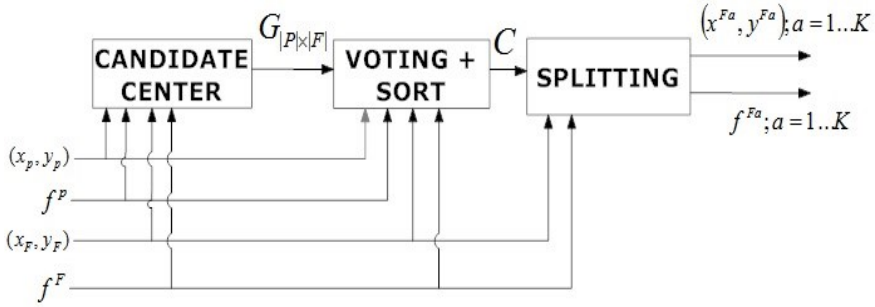

Fig. 2. Diagram of Step 1

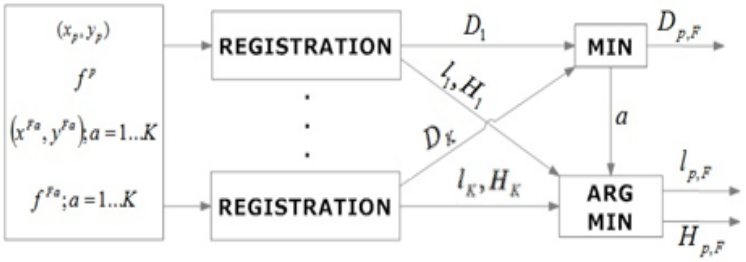

Fig. 3. Diagram of Step 2

small image is a partial image P and the larger one is a full image F. Both images are represented by their salient points, $(x^P, y^P) = \{(x_1^P, y_1^P), \ldots, (x_{|P|}^P, y_{|P|}^P)\}$ and $(x^F, y^F) = \{(x_1^F, y_1^F), \ldots, (x_{|F|}^F, y_{|F|}^F)\}$ together with their features $f^P = \{f_1^P, \ldots, f_{|P|}^P\}$ and $f^F = \{f_1^F, \ldots, f_{|F|}^F\}$. The number of salient points is $|P|$ and $|F|$, respectively.

In the first step, k positions (x_1^c, y_1^c), $\ldots, (x_k^c, y_k^c)$ on the full image F are selected as candidates to be the center of the partial image P if both images were aligned. Then, the full image F is split in sub-images $F_1, \ldots, F_k$, in which the center of each image F_a is the candidate position (x_a^c, y_a^c). Each split image F_a is represented by their set of salient points $(x^{Fa}, y^{Fa}) = \{(x_1^{Fa}, y_1^{Fa}),$

$\dots, (x^{F_a}_{|F_a|}, y^{F_a}_{|F_a|})\}$ and also their corresponding set of features $f^{F_a} = \{f^{F_a}_1, \dots, f^{F_a}_{|F_a|}\}$. Note that the number of extracted salient points in the partial image $|P|$ and the split ones $|F_a|$ can be different. Moreover, $|F| \leq \sum_{a=1}^{k} |F_a|$, since the split images can overlap.

In the second step, the algorithm seeks the best alignment between the salient points (x^P, y^P) of the partial image P and the salient points (x^{F_a}, y^{F_a}) of each of the split images $F_1, \dots, F_k$. To obtain these alignments, not only the salient point positions are used but also their extracted features, more precisely, features f^P and f^{F_a}. Thus, k distances $D_1, \dots, D_k$ and k alignments (also called homographies) $H_1, \dots, H_k$ are computed. Finally, the method selects the image that obtains the minimum distance and returns the alignment $H_{P,F}$ between P and F that obtains this distance. In the following subsections we will explain in a deeper way each of the two steps of our *PF-Registration* method.

2.1 Selecting Some Position Candidates

Figure 2 shows the main structure of the first step of our method. It is based on a Generalized Hough Transform [24, 25, 26]. As commented in the previous section, the method first obtains $|P|$ and $|F|$ salient points (position and features) of both images.

We define a $|P|$x$|F|$ matrix $\mathrm{G}[\mathrm{i},\mathrm{j}]$. The *Candidate Center* module fills each cell of $\mathrm{G}[\mathrm{i},\mathrm{j}]$ with the position (x^C_{ij}, y^C_{ij}) on the full image F that the center of the partial image $(\bar{x}, \bar{y})$ would obtain if the point (x^P_i, y^P_i) on the partial image was mapped to the point (x^F_j, y^F_j) on the full image. There are several forms to obtain these centers [26]. They can use only one or several points, and also some information extracted from the features, such as angle information. The aim of this process is to detect the spatial relations on both images. If s points in P and s points in F have the same relative position, then there are going to be s cells of $\mathrm{G}[\mathrm{i},\mathrm{j}]$ with the same value. These cells are such that the mapping between points on both images is the correct one. Notice that the complexity cost of this module is $O(|P| \cdot |F|)$ since this calculation depends solely on the number of salient points extracted in the partial image P and the full image F.

When the matrix G is filled, then the *Voting and Sort* module generates an ordered list C of the positions (x^C_{ij}, y^C_{ij}) found in G, where $C = \{(x^c_1, y^c_1), \dots, (x^c_T, y^c_T)\}$, through a clustering and voting process. List C is set in a descendent order. That is, the positions with the most votes are the first ones. Note that $T \leq |P|x|F|$. The voting process counts the number of centers grouped by the clustering process if their features are considered to be similar enough. The clustering process considers two center points (x^C_{ij}, y^C_{ij}) and $(x^C_{i'j'}, y^C_{i'j'})$ which have to be the same if they are close enough, that is, if the distance is lower than a spatial threshold defined by $dist^{position}_{P,M}\left((x^C_{ij}, y^C_{ij}), (x^C_{i'j'}, y^C_{i'j'})\right) < T_s$. Thus, the *Voting and Sort* module counts and orders the cells in G such that $dist^{position}_{P,M}\left((x^C_{ij}, y^C_{ij}), (x^C_{i'j'}, y^C_{i'j'})\right) < T_s$ and $dist^{feature}_{P,M}(f^F_i, f^P_j) < T_f$. Note that both distances are parameterized. In the case of $dist^{position}_{P,M}$, this is done to be independent of the rotation and scale. In the case of $dist^{feature}_{P,M}$, this is done to be independent of some global feature distortions. The computational complexity of this module is defined once again as $O(|P| \cdot |F|)$ since the process requires to find the best K candidates within G.

Finally, with these K candidates to be the center of the partial image on the full image, the set of points (x^F, y^F) and the set of features f^F are split in K point sets (x^{F_a}, y^{F_a}), $1 \leq a \leq K$, and K feature sets f^{F_a}, $1 \leq a \leq K$. Each point in (x^F_i, y^F_i) is included in the set F_a if $dist^{position}_{P,M}\left((x^F_i, y^F_i), (x^C_a, y^C_a)\right) \leq T_r$. The threshold T_r represents the maximum radius of the set, meaning the maximum distance between any point and the center of the set. Usually, it is determined depending on the radius of the partial set (x^P, y^P). The set f^{F_a} is defined congruent with the set (x^{F_a}, y^{F_a}). Parameter K is application dependent, but it is commonly set as a value equal or less than 4 to avoid spurious candidate centers. The complexity of this module is $O(K \cdot$

$|P|$), since the process is repeated K times and each F_a has, on average, $|P|$ salient points.

2.2 Best Candidate Selection through Multiple Correspondences

Figure 3 shows the second step of our registration method.

In this second step, the method first seeks the distances $D_a = dist(P, F_a);\ 1 \leq a \leq K$, and the correspondences l_a between the points in each set, and also the homographies H_a that transform P to F_a. Several algorithms can be used to find these correspondences and/or homographies. These algorithms use the positional information (x^{F_a}, y^{F_a}) and (x^P, y^P), and also their features f^{F_a} and f^P. For example, the Hungarian method [6] or its upgrade [7], ICP [5] (when no outliers are considered), RANSAC method [8] (which considers the presence of outliers), Bipartite Graph Matching [27] (which considers second order information), or more sophisticated ones [9] can be used. Even a greedy algorithm that simply selects the best option without considering the other candidates could be used. Notice that this module's computational complexity is dependent on the selected registration method. For example, we identify the complexity of using [6] as $O(K \cdot (2 \cdot |P|)^3)$.

We wish to select the set of points (x^{F_a}, y^{F_a}) that obtained the minimum distance D_a. This is because we assume D_a is a good enough approximation of $dist(P, F)$. Moreover, we also assume the correspondence and alignment (homography) between P and F approximates the correspondence l_a and homography H_a. Therefore, $l_{P,F} = l_a$ and $H_{P,F} = H_a$. There is no computational complexity involved in this module, since we simply select the minimum D_a and the corresponding l_a and H_a, a process that can be performed right after the Registration module.

Breaking down the full image in a set of candidates has two main advantages. On the one hand, the computational cost of obtaining the K distances D_a is lower than obtaining directly the value $D_{P,F}$. This is directly reflected as we notice a reduction in computational cost using our method compared to state of the art methods, where the whole full image has to be evaluated against the tiny one. On the other hand, the sub-optimal algorithm tends to obtain a more precise local minimum.

3 Validation

3.1 Dataset and Experimentation Process

We used images contained in the Tsinghua 500 PPI Palmprint Database [17]. It is a public high-resolution palmprint database composed of 500 palmprint images of 2040x2040 resolution and captured with a commercial palmprint scanner from Hisign. For this particular experimentation process, we selected the first 4 subjects of the database [28]. From each of these four subjects, eight images $I_1, I_2, \ldots, I_8$ of his or her palm are available, thus resulting in a total of 32 full images. For each subject, the first four images (I_1 through I_4 referred as TI_1 through TI_4 from now on) are kept in the Reference Set. The other four images (I_5 through I_8 referred as PI_1 through PI_4 from now on) are converted into small circular images c, each with a radius r, where $100 < r < 600$ pixels (consider $1\,pixel \cong 0.0264\,cm$). These circular samples conform our Test Set. In a real-life application, our Reference Set represents the full images possessed by an authority, and the Test Set represents the found palms, i.e., a sample taken from a crime scene. After the extraction method [17] is applied to each image, an average of 800 minutiae can be extracted from a full image, and an average of 50 minutiae can be extracted from a 100 pixel radius circular patch.

As explained in Section 2, when intending to find the correspondence of a small patch within a full image, the first step involves selecting, voting and splitting candidates. As a result of this step, we obtain the best partial candidate TI_a from a full palmprint in the reference set. In the second step, we calculate the matching between c and F_a, and the distance between the two is computed. This distance d is application dependent, and for our particular case is computed as $d(a_i^1, a_j^2) = \frac{1}{2} ad(\theta_i^1, \theta_j^2) + \frac{1}{2} dd((x,y)_i^1, (x,y)_j^2)$, where *ad* represents the angular distance and *dd* represents the Euclidean distance. When

Tables 1 and 2. Confusion matrix for c with r=100 pixels (left) and r=200 pixels (right) using the PF-Registration method

Confusion Matrix		Reference Set (T)			
		I1	I2	I3	I4
Test Set (P)	I1	0	0	4	0
	I2	1	3	0	0
	I3	1	0	2	1
	I4	1	1	1	1

Confusion Matrix		Reference Set (T)			
		I1	I2	I3	I4
Test Set (P)	I1	0	1	3	0
	I2	1	2	1	0
	I3	1	0	3	0
	I4	0	1	0	3

Tables 3 and 4. Confusion matrix for c with r=400 pixels (left) and r=600 pixels (right) using the PF-Registration method

Confusion Matrix		Reference Set (T)			
		I1	I2	I3	I4
Test Set (P)	I1	2	1	0	1
	I2	0	4	0	0
	I3	1	1	2	0
	I4	0	0	0	4

Confusion Matrix		Reference Set (T)			
		I1	I2	I3	I4
Test Set (P)	I1	4	0	0	0
	I2	0	4	0	0
	I3	0	0	4	0
	I4	0	0	0	4

comparing one matching with another, the one with the lowest distance is the one that reflects the correct identification.

3.2 Results

To show synthesized results, instead of presenting the whole table of comparisons between each circular patch and the whole reference set, we present the confusion matrices according to different radius sizes. Tables 1, 2, 3, and 4 show the confusion matrix for r=100, r=200, r=400, and r=600. The comparison of four different patches derived from different PI_i is performed with some elements contained in the database TI_i. With the previous knowledge that $PI_i = TI_i$, we then consider identification to be successful when the elements on the diagonal possess the highest similarity s of the whole row, where $s = 1/d$.

Tables 5 and 6. Confusion matrix for c with r=100 pixels (left) and r=200 pixels (right) using Hough method

Confusion Matrix		Reference Set (T)			
		I1	I2	I3	I4
Test Set (P)	I1	2	2	0	0
	I2	2	2	0	0
	I3	3	1	0	0
	I4	0	4	0	0

Confusion Matrix		Reference Set (T)			
		I1	I2	I3	I4
Test Set (P)	I1	1	3	0	0
	I2	1	3	0	0
	I3	1	3	0	0
	I4	0	3	0	1

Tables 7 and 8. Confusion matrix for c with r=400 pixels (left) and r=600 pixels (right) using Hough method

Confusion Matrix		Reference Set (T)			
		I1	I2	I3	I4
Test Set (P)	I1	1	3	0	0
	I2	0	4	0	0
	I3	0	2	2	0
	I4	0	2	0	2

Confusion Matrix		Reference Set (T)			
		I1	I2	I3	I4
Test Set (P)	I1	2	2	0	0
	I2	0	4	0	0
	I3	0	1	3	0
	I4	0	1	0	3

In Tables 5 to 8, we show the same confusion matrices computed for the same circular patches, this time using the Hough method, as proposed in [29].

Figure 4 shows a comparison between the recognition ratio of the classical Hough method versus the PF-Registration method. The Recognition Ratio reflects the percentage of times a circular patch is correctly matched with one of the image of the same individual in the Reference Set.

We observe that our method has a higher

Table 9. Runtime as the radius of the circular patch increases, for PF-Registration method (blue) and Hough method (red)

rad. [px]	100	200	300	400	500	600
PF-Re [hours]	0.3	0.7	3.9	20.2	39.9	66.2
Hough [hours]	24.1	30.2	80.6	129.9	171.6	249.9
Diff.	72.44	39.68	20.39	6.43	4.4	3.7

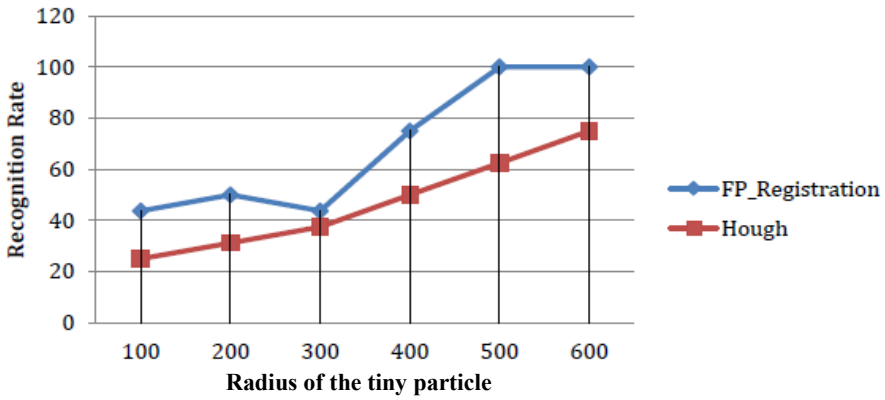

Fig. 4. Recognition Rate as the radius of the circular patch increases, for PF-Registration method (blue) and Hough method (red)

recognition rate than the Hough method for small images. Most notably, as the input image ratio is of about 100 pixels ($\cong 2.64$ cm), the increase of recognition is around 21%. It must be pointed out that when $r > 700$ pixels, both methods tend to have the same performance, arriving to the 100% recognition rate.

In Table 9 we present the runtime of the PF-Registration method compared to Hough method for the same experiments. Notice that as the size of the partial image increases, the difference between runtimes is smaller. Both of the methods have similar rates of change; nevertheless, our method seems to be faster than the classical one when the partial image is smaller. Thus, we present an option which is not only more accurate for small samples, but likewise faster in computational time.

4 Conclusions

Several algorithms have been presented to perform palmprint matching, achieving great accuracy rates and low computational complexity. These algorithms, useful in a wide range of applications (such as access validation or people identification), have the important drawback of not considering partial to full matching. In fields such as forensics, it is more usual to detect partial and noisy palmprints rather than a full sample. In this type of scenario, the standard algorithms suffer from important quality reduction or simply a lack of adaptability. For this reason, we have presented an algorithm for partial to full palmprint matching, which explicitly considers a noisy input image and a high outlier existence. Our algorithm is developed in such way that adapts the most basic principles of palmprint matching, but likewise is able to present a low computational complexity in a scalar form as the number of elements to be matched is reduced. In the experimental validation, we show that our method is effective, since we achieve a higher recognition ratio and a lower runtime compared to the state of the art classical method, as the ratio of the input image is reduced. Most notably, as the input image ratio is of about 100 pixels ($\cong 2.64$ cm), an increase of recognition of 21% with a runtime reduction of 72 times is obtained. Work still pending includes acquisition, adaptation, and experimentation with more samples or more palmprint databases, and an in depth comparison of our algorithm to methods like [16] or [17], which propose a solution to the same scenario that we work with.

Acknowledgements

This research is supported by the CICYT project DPI2013-42458-P, by project TIN2013-47245-C2-2-R, and by *Consejo Nacional de Ciencia y Tecnología* (CONACYT, Mexico).

References

1. **Salvi, J., Matabosch, C., Fofi, D., & Forest, J. (2007).** A review of recent range image registration methods with accuracy evaluation. *Image Vision Comput*., Vol. 25, No. 5, pp. 578–596.
2. **Ardeshir Goshtasby, A. (2005).** *2-D and 3-D Image Registration for Medical, Remote Sensing, and Industrial Applications*. Wiley Press.
3. **Zitová, B. & Flusser, J. (2003**). Image registration methods: a survey. *Image Vision Comput*., Vol. 21, No. 11, pp. 977–1000.
4. **Mikolajczyk, K. & Schmid, C. (2005**). A performance evaluation of local descriptors. *IEEE Trans. Pattern Anal. Mach. Intell.,* Vol. 27, No. 10, pp. 1615–1630.
5. **Zhang, Z. (1994).** Iterative point matching for registration of free-form curves and surfaces. *Int. J. Comput. Vision*, Vol. 13, No. 2, pp. 119–152.
6. **Kuhn, H.W. (1955).** The Hungarian method for the assignment problem Export. *Naval Research Logistics Quarterly*, Vol. 2, No. 1-2, pp. 83–97.
7. **Jonker, R. & Volgenant, T. (1986).** Improving the Hungarian Assignement Algorithm. *Operations Research Letters,* Vol. 5, No. 4, pp. 171–175.
8. **Fischler, M.A. & Bolles, R.C. (1981).** Random sample consensus: a paradigm for model fitting with applications to image analysis and automated cartography. *Commun. ACM*, Vol. 24, No. 6, pp. 381–395.
9. **Sanromà, G., Alquézar, R., Serratosa, F., & Herrera, B. (2012).** Smooth Point-set Registration using Neighbouring Constraints. *Pattern Recognition Letters*, Vol. 33, No. 15, pp. 2029–2037.
10. **Kokiopoulou, E. & Frossard, P. (2010).** Graph-based classification of multiple observation sets. *Pattern Recognition,* Vol. 43, No. 12, pp. 3988–3997.
11. **Wachinger, C. & Navab, N. (2013).** Simultaneous Registration of Multiple Images: Similarity Metrics and Efficient Optimization. *IEEE Trans. on Pattern Analysis and Matching Intelligence*, Vol. 35, No. 5, pp. 1221–1233.
12. **Somvanshi, P. & Rane, M. (2012).** Survey of Palmprint Recognition. *International Journal of Scientific & Engineering Research*, Vol. 3, No. 2.
13. **Zhang, D., Zuo, W., & Yue, F. (2012).** A Comparative Study of Palmprint Recognition Algorithms. *ACM Computing Surveys*, Vol. 44, No. 1, p. 2.
14. **Funada, J., Ohta, N., Mizoguchi, M., Temma, T., Nakanishi, K., Murai, A., Sugiuchi, T., Wakabayashi, T., & Yamada, Y. (1998).** Feature Extraction Method for Palmprint Considering Elimination of Creases. *Proc. of 14th Int. Conf. Pattern Recognition*, pp. 1849–1854.
15. **Kong, W.K. & Zhang, D. (2002).** Using Low-Resolution Palmprint Images and Texture Analysis for Personal Identification. *ICPR*.
16. **Jain, A.K. & Demirkus, M. (2008).** *On Latent Palmprint Matching*. MSU Technical Report.
17. **Jain, A.K. & Feng, J. (2009).** Latent Palmprint Matching. *IEEE Trans. on PAMI*.
18. **Dai, J. & Zhou, J. (2011**). Multifeature-Based High-Resolution Palmprint Recognition. *IEEE Trans. Pattern Analysis and Machine Intelligence*, Vol. 33, No. 5, pp. 945–957.
19. **Dai, J. & Zhou, J. (2012).** Robust and Efficient Ridge Based Palmprint Matching. *IEEE Transactions on Pattern Analysis and Matching Intelligence,* Vol. 34, No. 8, pp. 1618-1632.
20. **Wang, X., Liang, J., & Wang, M. (2013).** On-line fast palmprint identification based on adaptive lifting wavelet scheme. *Knowledge-Based Systems,* Vol. 42, pp. 68–73.
21. **Nibouche, O., Jiang, J. & Trundle, P. (2012).** Analysis of performance of palmprint matching with enforced sparsity. *Digital Signal Processing*, Vol. 22, No. 2, pp. 348–355.
22. **Badrinath, G.S. & Gupta, P. (2012).** Palmprint based recognition system using phase-difference information. *Future Generation Computer Systems*, Vol. 28, No. 1, pp. 287–305.
23. **Wang, X., Lei, L., & Wang, M. (2012).** Palmprint verification based on 2D Gabor wavelet and pulse-coupled neural network. *Knowledge-Based Systems*, Vol. 27, pp. 451–455.
24. **Jain, A.K., Flynn, P., & Ross, A. (2009).** *Handbook of Biometrics*. Springer.
25. **Ballard, D.H. (1980).** Generalizing the Hough Transform to Detect Arbitrary Shapes. Ridge Based Palmprint Matching. *IEEE Trans. on Pattern Analysis and Matching Intelligence*.
26. **Kassim, A.A., Tan, T., & Tan, K.H. (1999).** A comparative study of efficient generalised Hough transform techniques. *Image and Vision Computing,* Vol. 17, pp. 737–748.
27. **Serratosa, F. (2014).** Fast computation of bipartite graph matching. *Pattern Recognition Letters, Vol.* 45, pp. 244–250.
28. **Ratha, N.K., Karu, K., Chen, S., & Jain, A.K. (1996).** A Real-Time Matching System for Large

Fingerprint Databases. *IEEE Trans. on PAMI*, Vol. 18, No. 8, pp. 799–813.

Carlos Francisco Moreno García was born in Mexico City, Mexico, in 1988. He received his Master degree from Universitat Rovira i Virgili in 2012. He is currently a Ph.D. student at the same institution, where he collaborates with the Research group on Sensorial Systems Applied to the Industry (SSAI). His areas of interest are graphs, computer vision, pattern recognition, and machine learning, and his work includes developing applications of those areas in biometrics, information security, and biomedicine.

Francesc Serratosa was born in Barcelona, Spain, in 1967. He received his Ph.D. from Universitat Politecnica de Catalunya in 2000. He is currently a full professor of computer science at the Universitat Rovira i Virgili (Tarragona, Catalonia). Since 1993, he has been active in research in the areas of computer vision, robotics, structural pattern recognition, machine learning, and biometrics. He has published more than 100 papers and he is an active reviewer in some congresses and journals. He teaches computer vision and biometrics at Universitat Rovira i Virgily and Universitat Oberta de Catalunya. He is the principal researcher of the Research group on Sensorial Systems Applied to the Industry (SSAI).

Article received on 04/09/2014; accepted on 03/11/2014.